nature climate change

Article

https://doi.org/10.1038/s41558-026-02569-1

Emergence of Antarctic mineral resources in a warming world

Received: 23 June 2025

Accepted: 16 January 2026

Published online: 20 February 2026

Check for updates

Erica M. Lucas[1,2] ✉, Fred D. Richards[3], Gabriel Cederberg[4], Xiyuan Bao[4], Mark J. Hoggard[5], Stephen R. J. Tsuji[6], Konstantin Latychev[7], Leonard J. S. Tsuji[8] & Jerry X. Mitrovica[4]

The extent of ice-free land across Antarctica will increase in a warming world, driven by ice sheet retreat and sea-level change. Here we project an up to ~120,000 km^2 (~550%) increase in the extent of Antarctic ice-free land over the next three centuries, using a state-of-the-art sea level model combined with ice sheet melt predictions for a range of greenhouse gas emission scenarios. New ice-free land is projected to emerge in all regions with existing territorial claims as well as in the unclaimed sector in West Antarctica. The geologic setting and distribution of known mineral occurrences indicate that ice-free land emergence will expose new mineral deposits in these regions. With the likely rise in the economic viability of Antarctic mineral resources over the coming centuries, the environmental impacts of mineral resource extraction activities will be weighed against societal pressure for sustainable resource development.

The Antarctic Treaty was signed in 1959 by three categories of states: those with territorial claims in Antarctica (that is, Argentina, Australia, Chile, France, New Zealand, Norway and the United Kingdom; Fig. 1), non-claimant states (that is, Belgium, Japan and South Africa) and the USA and the Soviet Union (now Russia)[1]. Although seven states maintain territorial claims in Antarctica, many other countries do not recognize these claims[1–3]. Additionally, both the USA and Russia still maintain a basis to claim territory in Antarctica[1]. Article IV of the Antarctic Treaty asserts that nothing in the treaty renounces a state's previously asserted rights or territorial claims in Antarctica or prejudices a state's "recognition or non-recognition of any other State's right of or claim to territorial sovereignty in Antarctica"[1]. Only one sector of Antarctica remains unclaimed (Fig. 1). Furthermore, the Antarctic Treaty establishes Antarctica as a region reserved exclusively for scientific research and peaceful purposes[1].

At present, less than 0.6% (21,745–70,586 km^2) of Antarctica is estimated to be free of ice cover[4–6], with ice-free areas including coastal environments, mountain ranges, nunataks, valleys, islands and cliffs (Fig. 1). The Antarctic ice sheet has undergone rapid thinning and grounding-line retreat over the past few decades[7,8], and ice sheet retreat is expected to continue over the coming centuries[9]. This anthropogenically driven process will lead to the emergence of ice-free land (henceforth 'land') due to both the direct effect of ice margin retreat and the Earth system response to changes in ice loading—that is, glacial isostatic adjustment (GIA). Regarding the latter, at the margin of a rapidly melting ice sheet, sea level will fall due to the combined impact of post-glacial uplift and the loss of gravitational attraction between the ice and the surrounding oceans[10].

Land emergence in Antarctica over the coming centuries will have wide-ranging environmental impacts and implications for mineral resource development prospects, both of which will play key roles in shaping Antarctic geopolitics. Antarctica's terrestrial biodiversity is largely concentrated in ice-free areas[6,11,12], and these regions are also particularly important for geologic, fossil and soil sampling[13,14]. Furthermore, scientific research stations and associated infrastructure—including wharfs, roads and airfields[15]—are commonly built on

[1]Department of Earth and Planetary Sciences, McGill University, Montreal, Quebec, Canada. [2]Department of Earth and Planetary Sciences, University of California, Santa Cruz, Santa Cruz, CA, USA. [3]Department of Earth Science and Engineering, Imperial College London, London, UK. [4]Department of Earth and Planetary Sciences, Harvard University, Cambridge, MA, USA. [5]Research School of Earth Sciences, Australian National University, Canberra, Australian Capital Territory, Australia. [6]School of Environmental Studies, Queen's University, Kingston, Ontario, Canada. [7]Seakon, Toronto, Ontario, Canada. [8]Department of Physical and Environmental Sciences, and Department of Health and Society, University of Toronto, Toronto, Ontario, Canada. ✉e-mail: ericamlucas@gmail.com

https://doi.org/10.1038/s41558-026-02569-1

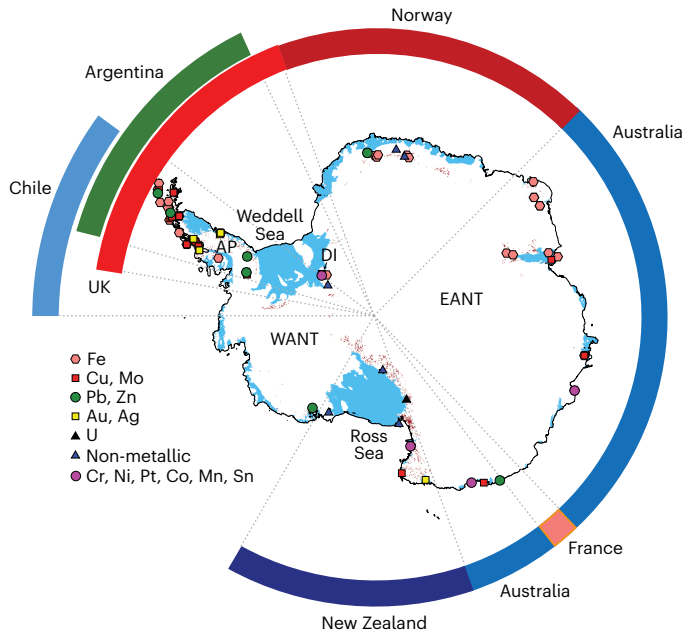

Fig. 1 | Territorial claims in Antarctica and known mineral occurrences. Grounded ice and ice shelves are shown in white and blue, respectively[65]. Rock outcrops are plotted in dark red[4]. West Antarctica (WANT), East Antarctica (EANT), the Antarctic Peninsula (AP) and the Dufek Intrusion (DI) are labelled. The symbols, with the legend at the bottom left, indicate known mineral occurrences[29].

land: 81% of buildings in Antarctica are located on ice-free land, with 76% concentrated in ice-free areas within just 5 km of the coast[5]. Research stations are known to substantially impact their surrounding environment through contamination, habitat damage and the introduction of non-native species[16–18]. Finally, with the growing demand for mineral resources[19–22], interest in mineral resource development of ice-free areas in Antarctica is likely to intensify[23–25].

The Protocol on Environmental Protection to the Antarctic Treaty (commonly known as the Madrid Protocol, or more precisely, the Environmental Protocol) provides the current framework for comprehensive environmental protection in Antarctica[26]. The Environmental Protocol—part of what has been called the Antarctic Treaty System—has two main objectives: to establish an environmental protection regime and prohibit all activities related to mineral resource development in Antarctica indefinitely. The Environmental Protocol does, however, allow for activities related to mineral resources if they are for scientific purposes (Article 7)[26].

Starting in 2048, any of the Antarctic Treaty Consultative Parties will be permitted to call for an Article 25 review conference of the Environmental Protocol[26]. At such a conference, proposed modifications or amendments "shall be adopted by a majority of the Parties, including 3/4 of the States which are Antarctic Treaty Consultative Parties at the time of adoption of this Protocol", and a "modification or amendment…shall enter into force upon ratification, acceptance, approval or accession by 3/4 of the Antarctic Treaty Consultative Parties, including ratification, acceptance, approval or accession by all States which are Antarctic Treaty Consultative Parties at the time of adoption of this Protocol" (Article 25)[26]. Furthermore, any change to the restriction on mineral resource activities in Article 7 will not go into effect unless a new binding legal regime has been ratified and entered into force (Article 25)[26].

Growing interest in the mineral resource potential of Antarctica may spur calls to modify the Environmental Protocol to allow mineral resource development or, alternatively, motivate state or non-state actors to disregard the protocol altogether[25,27,28]. An Article 25 review conference would also make it possible to review the Antarctic Treaty itself[1], which could be destabilizing to the entire Antarctic Treaty System[25]. To anticipate the nature of these issues, it is important to explore projections of the spatio-temporal pattern of land emergence and the mineral resource potential of Antarctica. To this end, we present projections of land emergence over the next three centuries. We focus on emergent land with potential mineral deposits and the connection of these regions to both claimed and unclaimed territories.

Resource potential of Antarctica

The current understanding of Antarctica's mineral resources remains limited; however, mineral occurrences identified in select ice-free regions across the continent have established the presence of potentially valuable deposits, including copper, iron, gold, silver, platinum and cobalt (Fig. 1)[29–31]. Insight into potential mineral deposits can be developed by considering both Antarctica's tectonic history and its lithospheric structure, which we consider below.

Antarctica had a central position in the Gondwanan sector of the Pangea supercontinent[32–36], and all continents that bordered Antarctica during this period host large mineral deposits, including South America, Africa, India and Australia[33]. Because these continents share a similar geologic architecture, it is reasonable to assume that comparable mineral deposits also exist in Antarctica[34]. The spatial distribution of mineral deposits is generally governed by a combination of geological factors, including tectonic setting, structural controls and the presence of certain lithologies[37]. Individual deposits are commonly part of larger mineralized belts that align with major structural features, such as orogenic fold belts, or are associated with specific lithological units, such as greenstone belts[37–39]. Several Phanerozoic fold belts in South America, Africa, India and Australia extend into Antarctica[35], and mineral belts associated with these structures are also likely to continue into Antarctica[32–34].

An example of such a continuation is found in the Transantarctic Mountains of northern Victoria Land. During the Palaeozoic era, Antarctica was located on the active palaeo-Pacific margin of Gondwana, and northern Victoria Land was, more specifically, located adjacent to southeastern Australia and New Zealand[30,35]. Mountain-building and hydrothermal events along this margin led to the formation of gold deposits[38,40]. The Dorn Gold Deposit located in northern Victoria Land has been linked to the same tectonic processes that produced gold provinces in Australia (New South Wales, Victoria and Tasmania) and New Zealand[30]. A second, important example of a geological continuation is the connection between the southern Andean margin of South America and the Antarctic Peninsula[35,36,41], which we return to below.

Potential mineral resources in Antarctica can also be inferred from existing constraints on solid Earth structure. Base metal deposits (copper, lead, zinc and nickel) and associated by-products are broadly classified as being either sediment-hosted or magmatic-hosted, depending on whether their formation is primarily associated with sedimentary processes or magmatic activity. Globally, it has been shown that 85% of sediment-hosted base metal deposits (including all that contain >10 Mt of metal) are located within 200 km of the transition between thick and regular continental lithosphere[42]. Likewise, magmatic processes have also been invoked as a mechanism that concentrates metals at the margins of thick lithosphere[43–45]. In Antarctica, substantial base metal deposits are therefore most likely to be located adjacent to the Transantarctic Mountain front, in select sectors of East Antarctica and offshore of the Antarctic Peninsula, all regions where transitions from thicker to thinner lithosphere occur (Fig. 2).

Although no proven oil or gas reserves have been identified in Antarctica, substantial resources are likely to exist in thick sedimentary basins offshore of the continent, including in the Ross Sea, the Weddell Sea and the East Antarctic margin[32,46,47].

https://doi.org/10.1038/s41558-026-02569-1

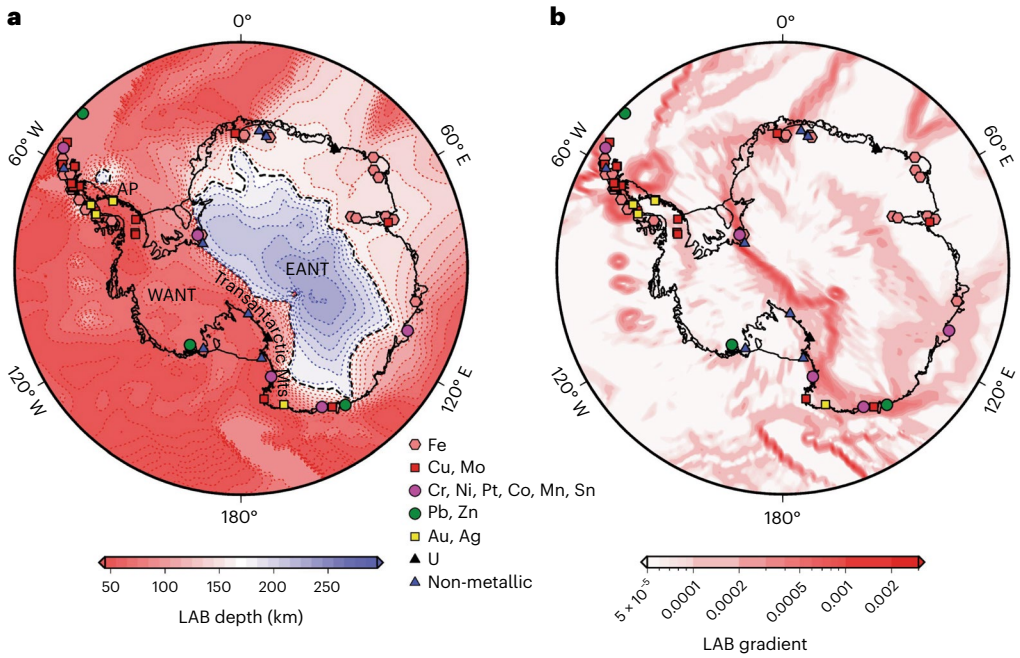

Fig. 2 | Lithospheric structure of Antarctica. a, Map of lithosphere–asthenosphere boundary (LAB) depth in Antarctica[66]. The black dashed line contours 170-km LAB thickness. **b**, LAB gradient map based on **a**. The symbols, with the legend at the bottom centre, indicate known mineral occurrences[29].

Ice-free land emergence

Over the next three centuries, land exposure will depend on the spatio-temporal pattern of ice sheet retreat and associated sea-level changes. To estimate land exposure over the coming centuries, we computed sea-level change for high, moderate and low ice melt projections using a high-resolution global GIA model that incorporates realistic, 3D variations in solid Earth structure[48–51] (Methods and Extended Data Fig. 1). The GIA model solves for gravitationally self-consistent sea-level changes for a specified space-time geometry of ice cover and a solid Earth viscoelastic structure model, accounting for both migrating shorelines and Earth rotational effects[52–54]. Because Greenland ice loss will contribute to future sea-level rise in Antarctica, we accounted for ice melt from both Antarctica and Greenland in computing sea-level change (Extended Data Fig. 2).

We predict that 120,610 km^2, 36,381 km^2 and 149 km^2 of new land will emerge in Antarctica by 2300 due to the combined effects of ice retreat and sea-level change for the high, moderate and low ice melt scenarios, respectively (Fig. 3, Extended Data Figs. 3 and 4 and Extended Data Table 1). The upper bound, corresponding to the high ice melt scenario, represents a ~550% increase in land relative to the estimate of present-day ice-free land (21,745 km^2) reported by Burton-Johnson et al.[4]. A 45,072 km^2 increase in land area is projected under the high ice melt scenario for 2200, and a 1,351 km^2 increase is projected for 2100.

Land emergence varies regionally over the next three centuries (Figs. 3 and 4 and Extended Data Figs. 3–5). Land emergence is largest in West Antarctica over the remainder of this century; that region is projected to gain 1,013 km^2 of land by 2100 in the high ice melt scenario (Fig. 3a). By 2200, land gains in the Antarctic Peninsula (37,535 km^2) far surpass those in West Antarctica (3,763 km^2) for the high ice melt scenario, and by 2300, land emergence reaches 75,510 km^2 in the Antarctic Peninsula (Figs. 3 and 4b). Widespread land gains also occur in coastal East Antarctica in this case, particularly between Enderby Land and Queen Mary Land (Fig. 4c), reaching 16,819 km^2 by 2300. Our results indicate that an average regional ice thinning of ~200–300 m is sufficient to expose tens of thousands of square kilometres of new land in a given region.

Including the effects of sea-level change in land gain estimates results in larger projections of ice-free areas than estimates based on ice sheet retreat alone (Figs. 3 and 4 and Extended Data Figs. 3–5). For the high ice melt scenario, 21% of the new land exposed by 2150 results from sea-level change (Fig. 3d). Under the moderate ice melt scenario, the relative contribution of sea-level change to land exposure peaks in 2200, accounting for 18% of the land gain (Extended Data Fig. 3b,d). Finally, in the low ice melt scenario, 74% of the land exposed in 2300 results from sea-level change (Extended Data Fig. 4). At the local scale, accounting for sea-level change in projections of land emergence can cause smaller ice-free areas to coalesce into larger ones, often resulting in the formation of larger islands or peninsulas (Fig. 4), as has been shown in other marine areas of the world[55]. Despite the overall expansion in ice-free area, some regions experience localized land loss due to ice sheet advance or sea-level rise. For example, in the high ice melt scenario, up to 613 km^2 of land loss in such regions is predicted to occur by 2300.

Land emergence in claimed territories

The emergence of land over the coming centuries may influence the willingness of Antarctic Treaty states, including those with and without territorial claims, to advocate for mineral resource development in Antarctica. The largest land emergence across the continent is projected to occur in the sector of the Antarctic Peninsula that is claimed by Argentina, Chile and the United Kingdom, with 36,043 km^2 of land gain by 2200 and 70,992 km^2 by 2300 for the high ice melt scenario (Sector 8 in Fig. 5). The analogous figures for the moderate ice melt scenario are 2,776 km^2 and 33,542 km^2 (Extended Data Fig. 6). In contrast, 14 km^2 of land loss is projected in the same sector for the low ice melt scenario by 2300 (Extended Data Fig. 7). The sector of the Antarctic Peninsula claimed by Argentina, Chile and the United Kingdom hosts a broad range of known mineral occurrences (Fig. 1), including copper, gold, silver and iron, suggesting that land emergence will expose new deposits (Fig. 6).

Because our understanding of Antarctica's mineral resources remains limited, known mineral occurrences in the Antarctic Peninsula cannot be taken as reliable indicators of the size of unknown

https://doi.org/10.1038/s41558-026-02569-1

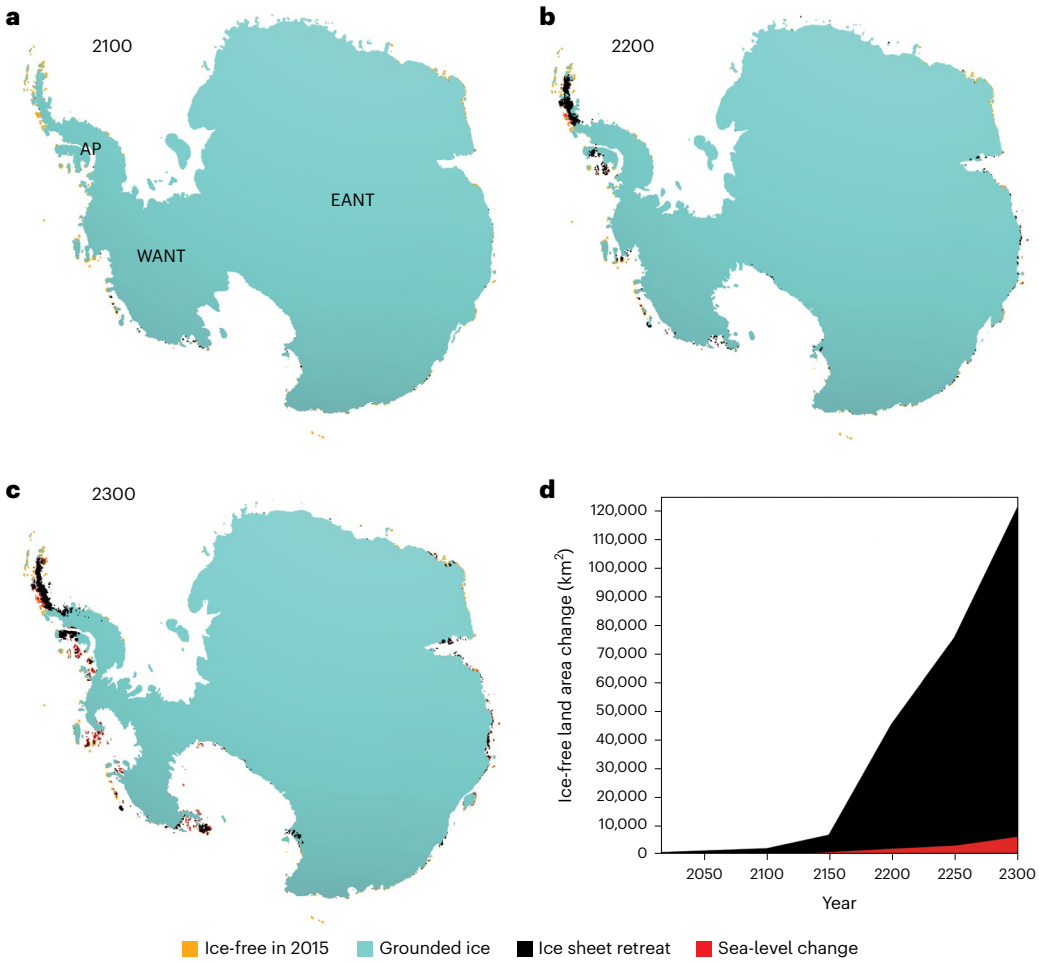

Fig. 3 | Land emergence for the high ice melt scenario. a–**c**, Projections of ice-free land area change due to ice sheet retreat and sea-level change for 2100, 2200 and 2300. Land area in 2015, calculated from the initial ice sheet extent of the adopted ice sheet model and high-resolution bedrock topography, is plotted in yellow ('Ice-free in 2015'). Note that we did not plot ice-free land observed at present as shown in Fig. 1; we only plotted the change in ice-free land exposure due to ice sheet retreat and associated sea-level change. The extent of grounded ice in 2100, 2200 and 2300 is shown in blue (see legend). **d**, Total ice-free land change from 2015 through 2300. The contributions from ice sheet retreat and sea-level change are plotted in black and red, respectively. Figure 4 provides higher-resolution plots for select regions for 2300. Extended Data Figs. 3 and 4 provide plots of land emergence for the moderate and low ice melt scenarios.

deposits. A better, albeit imperfect, measure of the latter can be based on a comparison with known mineral deposits in the Andean margin of South America, a magmatic arc that shares a geological history with the Antarctic Peninsula[35,36,41]. As an example, we estimated the amount of porphyry-hosted copper in the Antarctic Peninsula on the basis of the size of published porphyry-copper deposits in the Andean margin. Using geological province boundaries[56] and a global compilation of porphyry deposits[42], our analysis indicates ~420 Mt of porphyry-hosted copper distributed over ~1.2 million km^2 in the Andean margin, corresponding to ~350 tonnes of copper per square kilometre. Therefore, our estimates cited above of land gain in the Antarctic Peninsula by 2300 for the high and moderate ice melt scenarios, 70,992 km^2 and 33,542 km^2, respectively, yield estimates of ~24.8 Mt and ~11.7 Mt of porphyry-hosted copper within this newly exposed region. As a final point, we note that transitions from thinner to thicker lithosphere also occur in this region, raising the possibility of other mineralization styles[42] (Figs. 1 and 2).

The Dufek Intrusion, a large layered mafic intrusion similar in structure to the Stillwater Complex (USA) and the Bushveld Complex (South Africa)[57,58], is also situated in the territory claimed by Argentina, Chile and the United Kingdom (Fig. 1). Layered mafic intrusions such as the Dufek Intrusion are of global interest for their potential to host platinum group elements[43]. For example, ~70% of the world's platinum is currently mined from the Bushveld Complex[59]. While our projections show limited land emergence in the Dufek Intrusion region by 2300, the projected retreat of the Filchner–Ronne Ice Shelf[9] and widespread land emergence on the nearby Antarctic Peninsula may enhance the logistical feasibility of mineral resource development in the region (Figs. 5 and 6).

Beyond the Antarctic Peninsula, notable land emergence is projected in territories claimed by Australia (16,843 km^2 gain by 2300) and New Zealand (13,511 km^2 gain by 2300) for the high ice melt scenario (Fig. 5 and Extended Data Table 2). Copper and iron are the primary metals that have been identified in Australia's claimed territory to date (Fig. 1). Continued land emergence may also expose new, potentially valuable mineral resources in the region. For example, New Zealand's claimed territory is situated near a strong transition in lithospheric thickness along the Transantarctic Mountains front, making it possible that new mineral deposits will be exposed in the region by 2300[42] (Fig. 2). Finally, the Dorn Gold Deposit is located in the territory claimed by New Zealand[30], yet minimal land emergence is projected to occur near the location of the deposit (Fig. 6).

Up to 14,315 km^2 of land is projected to emerge in the unclaimed territory in West Antarctica by 2300 in the high ice melt scenario (Fig. 5). Ice sheet retreat and sea-level change will lead to widespread land emergence throughout the West Antarctic region, including the

https://doi.org/10.1038/s41558-026-02569-1

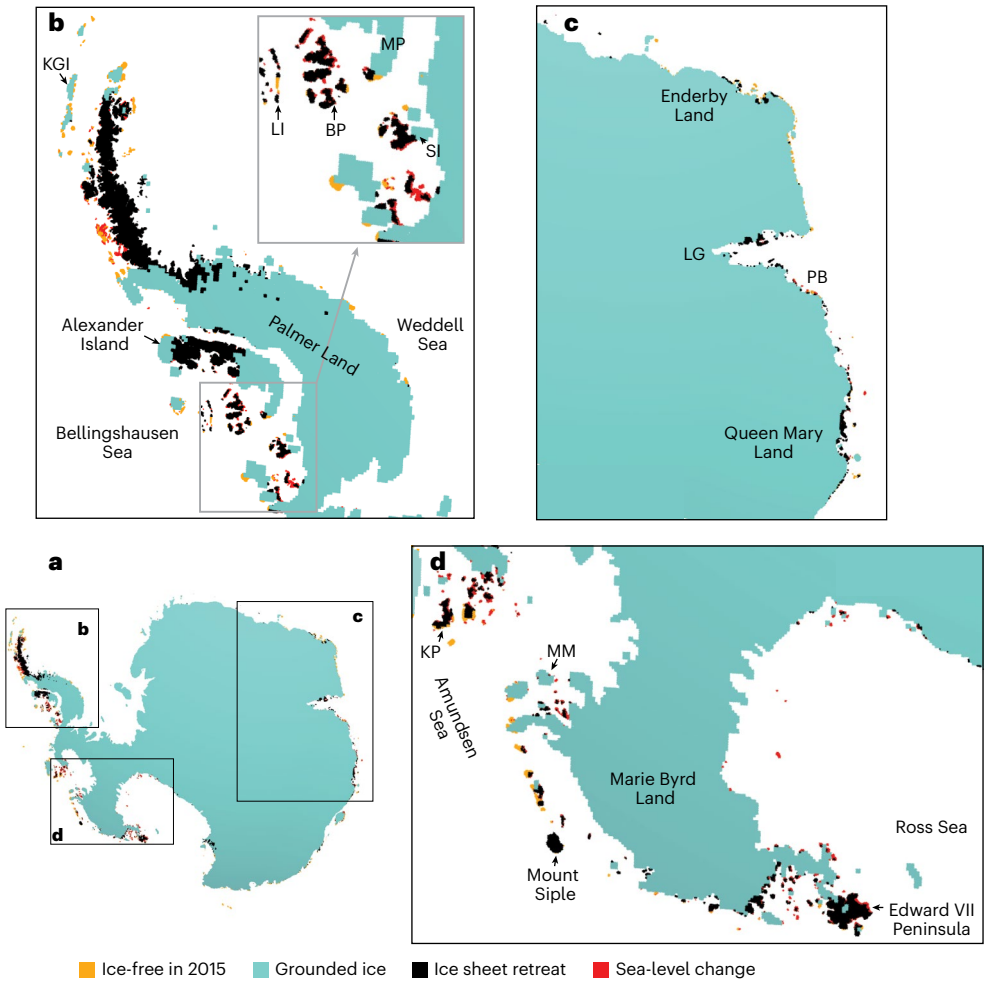

Fig. 4 | Regional-scale view of land emergence in 2300 for the high ice melt scenario. a, Map delineating the regions shown in **b**–**d**. **b**, Land emergence in the Antarctic Peninsula in 2300. The labelled geographic features include King George Island (KGI), Beethoven Peninsula (BP), Monteverdi Peninsula (MP), Latady Island (LI) and Spaatz Island (SI). **c**, Land emergence in a coastal sector of East Antarctica, with the Lambert Graben (LG) and Prydz Bay (PB) labelled. **d**, Land emergence in the Ross Sea, Marie Byrd Land and Amundsen Sea sectors of West Antarctica. The labelled geographic features include Mount Murphy (MM) and King Peninsula (KP). Extended Data Figs. 4 and 5 provide analogous plots for the low and moderate ice melt scenarios.

development of many new small islands in the Amundsen Sea and Ross Sea sectors (Fig. 4d). Given the region's prolonged history of rifting and magmatism from the early Jurassic through the present[36,60,61], this unclaimed territory is prospective for various types of deposits.

In addition to exposing new mineral resources, projected land emergence and ice shelf retreat will probably ease challenges to hydrocarbon exploration and exploitation in Antarctica's thick sedimentary basins. These include prospective hydrocarbon deposits in the Weddell Sea, Ross Sea and Bellingshausen Sea and near Prydz Bay[32,46,47]—all areas that fall within territories claimed by Argentina, Australia, Chile, New Zealand and the United Kingdom (Fig. 5).

Discussion

With the accelerating global demand for critical mineral resources[62], Antarctic land emergence over the next three centuries may spark increased interest in mineral resource development on the continent. Newly exposed land will almost certainly reveal previously unidentified mineral deposits. Moreover, by increasing areas suitable for constructing infrastructure, land emergence will also reduce formidable logistical barriers that are currently limiting the economic viability of mineral resource development in Antarctica. A given state's interest in advocating for mineral resource development may be linked to whether it holds a territorial claim, the economic value of mineral resources within that claimed territory and the extent of land emergence. However, this interest may also come from states without territorial claims or non-state actors. Geopolitical tensions are likely to rise with increasing land emergence, particularly concerning areas such as the Antarctic Peninsula and Weddell Sea sector, where territorial claims by Argentina, Chile and the United Kingdom overlap.

Since 1998, the Environmental Protocol has prohibited all activities related to mineral resource development in Antarctica. However, looking ahead—especially to 2048, when Consultative Parties to the Antarctic Treaty will be permitted to call for a review of the Environmental Protocol—the question of mineral resource development in Antarctica is likely to energetically resurface. Antarctica remains the only continent on which mineral resource extraction has not occurred. Whether this continues to be the case, and whether the spirit and intent of the Environmental Protocol remain intact, will be a complex issue. Although the commercial viability of mineral resource development in Antarctica remains uncertain due to its remoteness and extreme environmental conditions[25,63], the success of Arctic mining and hydrocarbon operations demonstrates that resource extraction in polar environments can be economically viable and technically feasible[64]. In a warming world, where emergent mineral resources in Antarctica may become economically viable, the substantial environmental impacts of mineral exploitation will be weighed against the necessity

https://doi.org/10.1038/s41558-026-02569-1

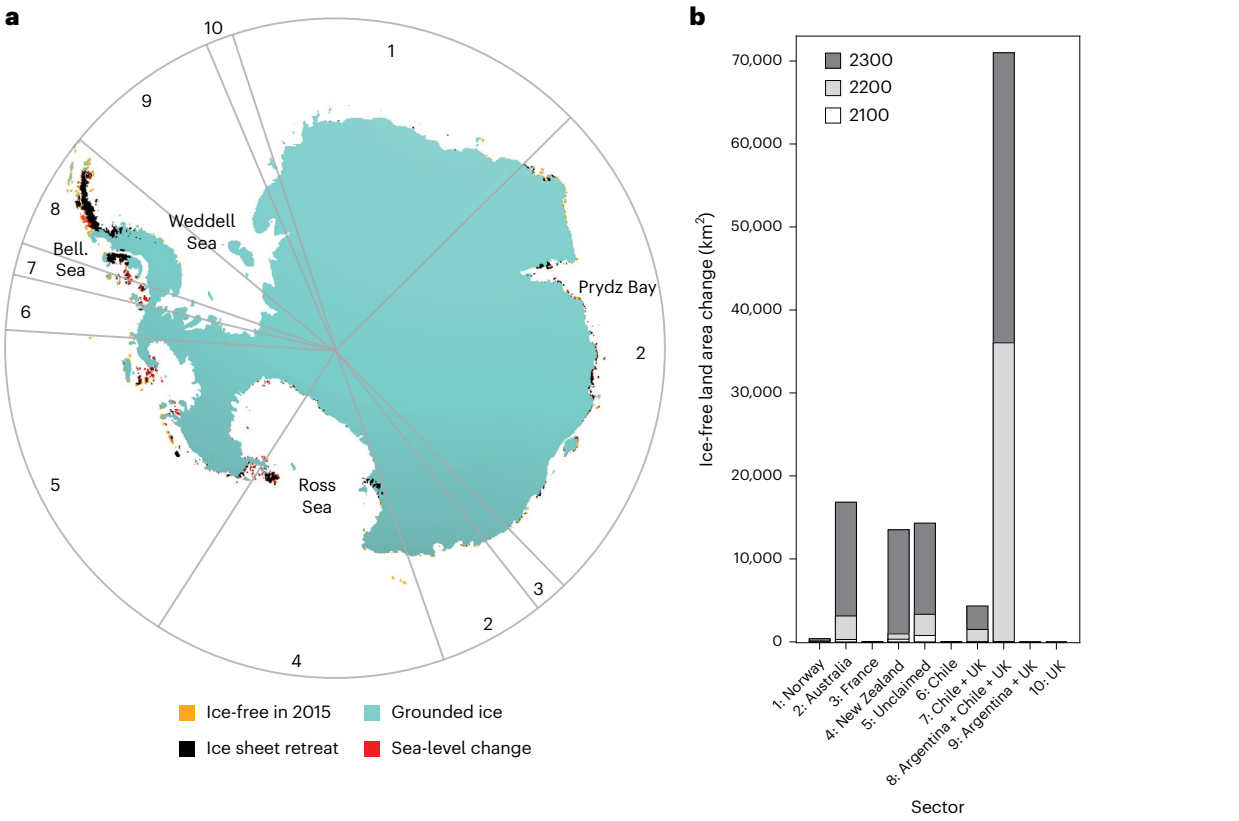

Fig. 5 | Land emergence in claimed territories for the high ice melt scenario. **a**, Land exposed in 2300 for the high ice melt scenario. The grey lines delineate sectors with territorial claims; the numbers 1 through 10 correspond to the countries or groups of countries labelled in the bar chart in **b**. Bellingshausen is abbreviated as 'Bell.' **b**, Land emergence by sector for 2100, 2200 and 2300. Extended Data Figs. 6 and 7 show analogous plots for the moderate and low ice melt scenarios.

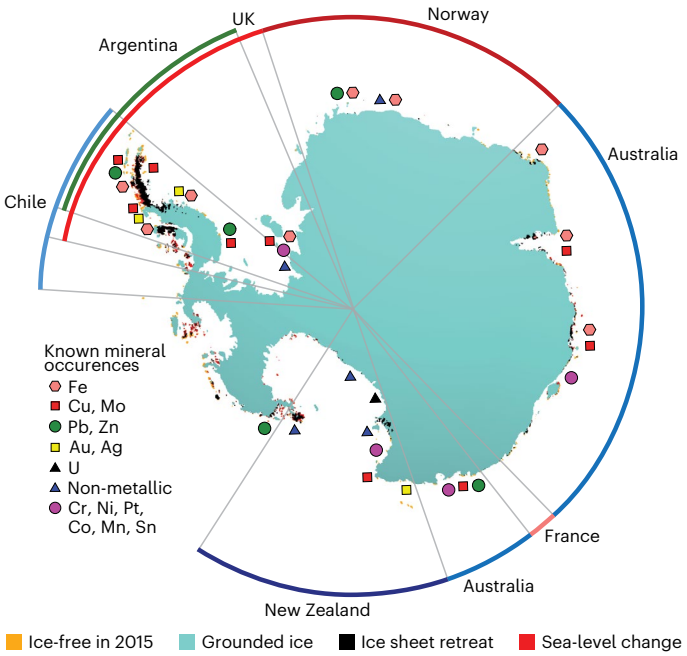

Fig. 6 | Land emergence, territorial claims and known mineral occurrences. Land exposed in 2300 for the high ice melt scenario shown together with territorial claims and known mineral occurrences[29]. For visual clarity, known mineral occurrences are plotted near, but not exactly at, their known locations. The exact locations of known mineral occurrences are shown in Fig. 1.

of developing mineral deposits important for sustainable development and the clean energy transition.

Online content

Any methods, additional references, Nature Portfolio reporting summaries, source data, extended data, supplementary information, acknowledgements, peer review information; details of author contributions and competing interests; and statements of data and code availability are available at https://doi.org/10.1038/s41558-026-02569-1.

References

1. *The Antarctic Treaty* (Antarctic Treaty Secretariat, 1959).
2. Thorp, A. *Antarctica: The Treaty System and Territorial Claims* (House of Commons Library, 2012).
3. Antarctica. In *The World Factbook* (Central Intelligence Agency, 2025).
4. Burton-Johnson, A., Black, M., Fretwell, P. T. & Kaluza-Gilbert, J. An automated methodology for differentiating rock from snow, clouds and sea in Antarctica from Landsat 8 imagery: a new rock outcrop map and area estimation for the entire Antarctic continent. *Cryosphere* **10**, 1665–1677 (2016).
5. Brooks, S. T. et al. Our footprint on Antarctica competes with nature for rare ice-free land. *Nat. Sustain.* **2**, 185–190 (2019).
6. Tóth, A. B. et al. A dataset of Antarctic ecosystems in ice-free lands: classification, descriptions, and maps. *Sci. Data* **12**, 133 (2025).
7. Rignot, E. et al. Four decades of Antarctic ice sheet mass balance from 1979–2017. *Proc. Natl Acad. Sci. USA* **116**, 1095–1103 (2019).

8. Shepherd, A. et al. Trends in Antarctic ice sheet elevation and mass. *Geophys. Res. Lett.* **46**, 8174–8183 (2019).
9. Seroussi, H. et al. Evolution of the Antarctic ice sheet over the next three centuries from an ISMIP6 model ensemble. *Earth's Future* **12**, e2024EF004561 (2024).
10. Farrell, W. E. & Clark, J. A. On postglacial sea level. *Geophys. J. Int.* **46**, 647–667 (1976).
11. Chown, S. L. & Convey, P. Spatial and temporal variability across life's hierarchies in the terrestrial Antarctic. *Phil. Trans. R. Soc. B* **362**, 2307–2331 (2007).
12. Lee, J. et al. Climate change drives expansion of Antarctic ice-free habitat. *Nature* **547**, 49–54 (2017).
13. O'Neill, T. A. Protection of Antarctic soil environments: a review of the current issues and future challenges for the Environmental Protocol. *Environ. Sci. Policy* **76**, 153–164 (2017).
14. Cox, S. C. et al. A continent-wide detailed geological map dataset of Antarctica. *Sci. Data* **10**, 250 (2023).
15. *Antarctic Station Catalogue* (Council of Managers of National Antarctic Programs, 2017).
16. Tin, T. et al. Impacts of local human activities on the Antarctic environment. *Antarct. Sci.* **21**, 3–33 (2009).
17. Aronson, R. B., Thatje, S., McClintock, J. B. & Hughes, K. A. Anthropogenic impacts on marine ecosystems in Antarctica. *Ann. N. Y. Acad. Sci.* **1223**, 82–107 (2011).
18. Brooks, S. T., Jabour, J., Sharman, A. J. & Bergstrom, D. M. An analysis of environmental incidents for a national Antarctic program. *J. Environ. Manage.* **212**, 340–348 (2018).
19. National Research Council *Minerals, Critical Minerals, and the U.S. Economy* (National Academies Press, 2008).
20. Watari, T., Nansai, K. & Nakajima, K. Review of critical metal dynamics to 2050 for 48 elements. *Resour. Conserv. Recycl.* **155**, 104669 (2020).
21. Vidal, O., le Boulzec, H., Andrieu, B. & Verzier, F. Modelling the demand and access of mineral resources in a changing world. *Sustainability* **14**, 11 (2022).
22. *Global Critical Minerals Outlook 2025* (IEA, 2025).
23. Foster, C. E. in *Antarctic Security in the Twenty-First Century: Legal and Policy Perspectives* (eds Hemmings, A. D. et al.) 154–171 (Routledge, 2012).
24. Rintoul, S. R. et al. Choosing the future of Antarctica. *Nature* **558**, 233–241 (2018).
25. Press, A. J. & Jackson, A. W. in *Geopolitical Change and the Antarctic Treaty System* (eds Scott, S. V. et al.) 231–248 (Springer Polar Sciences, 2024).
26. *Protocol on Environmental Protection to the Antarctic Treaty* (Antarctic Treaty Secretariat, 1991).
27. Liggett, D., Frame, B., Gilbert, N. & Morgan, F. Is it all going south? Four future scenarios for Antarctica. *Polar Rec.* **53**, 459–478 (2017).
28. Runde, D. F. & Zeimer, H. *Great Power Competition Comes for the South Pole* (Center for Strategic and International Studies, 2023).
29. Guild, P. W. et al. *Explanatory Notes for the Mineral-Resources Map of the Circum-Pacific Region: Antarctica Sheet* (US Geological Survey, 1998).
30. Crispini, L., Federico, L., Capponi, G. & Talarico, F. The Dorn gold deposit in northern Victoria Land, Antarctica: structure, hydrothermal alteration, and implications for the Gondwana Pacific margin. *Gondwana Res.* **19**, 128–140 (2011).
31. Yaxley, G. et al. The discovery of kimberlites in Antarctica extends the vast Gondwanan Cretaceous province. *Nat. Commun.* **4**, 2921 (2013).
32. Behrendt, J. C. in *Petroleum and Mineral Resources of Antarctica* (ed. Behrendt, J. C.) 3–24 (US Geological Survey, 1983).
33. Craddock, C. in *Mineral Resources Potential of Antarctica* (eds Splettstoesser, J. F. & Dreschhoff, G. A. M.) 1–6 (American Geophysical Union, 1990).
34. Wilsher, W. A. & de Wit, M. J. in *Mineral Resources Potential of Antarctica* (eds Splettstoesser, J. F. & Dreschhoff, G. A. M.) 7–14 (American Geophysical Union, 1990).
35. Boger, S. D. Antarctica—before and after Gondwana. *Gondwana Res.* **19**, 335–371 (2011).
36. Jordan, T. A., Riley, T. R. & Siddoway, C. S. The geological history and evolution of West Antarctica. *Nat. Rev. Earth Environ.* **1**, 117–133 (2020).
37. Robb, L. *Introduction to Ore-Forming Processes* 2nd edn (Wiley-Blackwell, 2020).
38. Goldfarb, R. J., Groves, D. I. & Gardoll, S. Orogenic gold and geologic time: a global synthesis. *Ore Geol. Rev.* **18**, 1–75 (2001).
39. Groves, D. I., Vielreicher, R. M., Goldfarb, R. J. & Condie, K. C. in *Mineral Deposits and Earth Evolution* (eds McDonald, I. et al.) 71–101 (Geological Society of London, 2005).
40. Bierlein, F. P., Christie, A. B. & Smith, P. K. A comparison of orogenic gold mineralisation in central Victoria (AUS), western South Island (NZ) and Nova Scotia (CAN): implications for variations in the endowment of Palaeozoic metamorphic terrains. *Ore Geol. Rev.* **25**, 125–168 (2004).
41. Saunders, A. D. & Tarney, J. Igneous activity in the Southern Andes and northern Antarctic Peninsula: a review. *J. Geol. Soc. Lond.* **139**, 691–700 (1982).
42. Hoggard, M. J. et al. Global distribution of sediment-hosted metals controlled by craton edge stability. *Nat. Geosci.* **13**, 504–510 (2020).
43. Begg, G. C. et al. Lithospheric, cratonic, and geodynamic setting of Ni-Cu-PGE sulfide deposits. *Econ. Geol.* **105**, 1057–1070 (2010).
44. Griffin, W., Begg, G. & O'Reilly, S. Continental-root control on the genesis of magmatic ore deposits. *Nat. Geosci.* **6**, 905–910 (2013).
45. Chen, C. et al. Sulfide-rich continental roots at cratonic margins formed by carbonated melts. *Nature* **637**, 615–621 (2025).
46. Kingston, J. *The Undiscovered Oil and Gas of Antarctica* Open File Report No. 91-597 (US Geological Survey, 1991).
47. Galushkin, Y. I., Leichenkov, G. L. & Dubinin, E. P. Hydrocarbon generation by the rocks of the Bremer Formation in adjacent areas of the nonvolcanic passive margins of Australia and Antarctica. *Geochem. Int.* **56**, 554–565 (2018).
48. Latychev, K. et al. Glacial isostatic adjustment on 3-D Earth models: a finite-volume formulation. *Geophys. J. Int.* **161**, 421–444 (2005).
49. Gomez, N., Latychev, K. & Pollard, D. A coupled ice sheet–sea level model incorporating 3D Earth structure: variations in Antarctica during the last deglacial retreat. *J. Clim.* **31**, 4041–4054 (2018).
50. Greve, R. & Chambers, C. Mass loss of the Greenland ice sheet until the year 3000 under a sustained late-21st-century climate. *J. Glaciol.* **68**, 618–624 (2022).
51. Greve, R. et al. Future projections for the Antarctic ice sheet until the year 2300 with a climate-index method. *J. Glaciol.* **69**, 1569–1579 (2023).
52. Kendall, R. A., Mitrovica, J. X. & Milne, G. A. On post-glacial sea level—II. Numerical formulation and comparative results on spherically symmetric models. *Geophys. J. Int.* **161**, 679–706 (2005).
53. Mitrovica, J. X., Wahr, J., Matsuyama, I. & Paulson, A. The rotational stability of an ice-age Earth. *Geophys. J. Int.* **161**, 491–506 (2005).
54. Mitrovica, J. X. & Milne, G. A. On post-glacial sea level: I. General theory. *Geophys. J. Int.* **154**, 253–267 (2003).
55. Tsuji, L. J. S., Gomez, N., Mitrovica, J. X. & Kendall, R. Post-glacial isostatic adjustment and global warming in subarctic Canada: implications for islands of the James Bay region. *Arctic* **62**, 458–467 (2009).
56. Hasterok, D. et al. New maps of global geological provinces and tectonic plates. *Earth Sci. Rev.* **231**, 104069 (2022).

57. Ford, A. B. *Stratigraphy of the Layered Gabbroic Dufek Intrusion, Antarctica* Geological Survey Bulletin No. 1405-D (US Geological Survey, 1976).
58. Jordan, T. A. & Riley, T. R. Reinvestigating the Dufek Intrusion, through joint gravity and magnetic models. *Phys. Earth Planet. Inter.* **356**, 107268 (2024).
59. *Mineral Commodity Summaries 2024* (US Geological Survey, 2024).
60. Wilch, T. I., McIntosh, W. C. & Panter, K. S. in *Volcanism in Antarctica: 200 Million Years of Subduction, Rifting and Continental Break-Up* (eds Smellie, J. L. et al.) 515–576 (Geological Society, 2021).
61. Lucas, E. M., Nyblade, A. A., Wiens, D. A., Aster, R. C. & Wilson, T. J. Seismic evidence for widespread active magmatism in eastern Marie Byrd Land, Antarctica. *Geophys. Res. Lett.* **52**, e2025GL116647 (2025b).
62. Rowan, L. R. *Critical Mineral Resources: National Policy and Critical Minerals List* Report No. R47982 (Congressional Research Service, 2025).
63. Grob, J. Antarctica's frozen territorial claims: a meltdown proposal. *Boston College Int. Comp. Law Rev.* **30**, 461–484 (2007).
64. Talalay, P. G. & Zhan, N. Antarctic mineral resources: looking to the future of the Environmental Protocol. *Earth Sci. Rev.* **232**, 104142 (2022).
65. Mouginot, J., Scheuchl, B. & Rignot, E. *MEaSUREs Antarctic Boundaries for IPY 2007–2009 from Satellite Radar, Version 2* (NASA National Snow and Ice Data Center Distributed Active Archive Center, 2017).
66. An, M. et al. Temperature, lithosphere–asthenosphere boundary, and heat flux beneath the Antarctic Plate inferred from seismic velocities. *J. Geophys. Res. Solid Earth* **120**, 8720–8742 (2015).

Publisher's note Springer Nature remains neutral with regard to jurisdictional claims in published maps and institutional affiliations.

Springer Nature or its licensor (e.g. a society or other partner) holds exclusive rights to this article under a publishing agreement with the author(s) or other rightsholder(s); author self-archiving of the accepted manuscript version of this article is solely governed by the terms of such publishing agreement and applicable law.

© The Author(s), under exclusive licence to Springer Nature Limited 2026

Methods

GIA modelling

The GIA model used in this study requires two key inputs: a viscoelastic Earth model and a model of spatio-temporal variations in ice cover (that is, an ice model). The Earth model includes an elastic lithosphere with variable thickness and a mantle with laterally varying viscosity (Extended Data Fig. 1). Variations in lithospheric thickness are based on the model of An et al.[66] in Antarctica and the model of Conrad and Lithgow-Bertelloni[67] globally (Extended Data Fig. 1). Lithospheric thickness is scaled to have an average value of 96 km in Antarctica, with a minimum thickness of 40 km (ref. 68). Mantle viscosity variations[69] are based on the ANT-20 shear-wave seismic model[70] for the upper mantle beneath Antarctica and the GLAD-M25 shear wave model[71] across the rest of the globe (Extended Data Fig. 1). Variations in mantle viscosity are estimated from relative variations in seismic velocity[48,72]. Mantle viscosity variations are superimposed on a one-dimensional reference viscosity profile, which has viscosities of 5×10^{20} Pa s and 5×10^{21} Pa s in the upper and lower mantle, respectively. The elastic and density structure of the Earth model varies radially and is based on the STW105 seismic tomography model[73]. GIA simulations were performed on a global tetrahedral grid with a surface resolution of 3–4 km over Antarctica and Greenland and 12–15 km elsewhere using the Seakon GIA model[48], revised to allow for lateral grid refinement and composite Earth models[49].

We computed relative sea-level changes for low, moderate and high ice melt scenarios using output from SICOPOLIS ice sheet model simulations[50,51,74]. The ice melt scenarios are adopted from Antarctic and Greenland ice sheet simulations forced with either Coupled Model Intercomparison Project Phase 5 (CMIP5) or CMIP6 oceanic and atmospheric conditions[75] from 2015 to 2100[76,77] extended to 2300 using a sustained late-twenty-first-century climate forcing for Greenland[50] and a climate-index method for Antarctica[51]. The low ice melt scenario combines Antarctic and Greenland ice sheet simulations forced by the low-emission Representative Concentration Pathway 2.6 (CMIP5) / Shared Socioeconomic Pathway 1-2.6 (CMIP6) pathway[50,51]. Under the low ice melt scenario, Antarctica and Greenland respectively contribute ~13 cm and ~8 cm to global mean sea-level rise by 2300. The moderate and high ice melt scenarios combine Antarctic and Greenland ice sheet simulations forced by the high-emission Representative Concentration Pathway 8.5 (CMIP5) / Shared Socioeconomic Pathway 5-8.5 (CMIP6) pathway[50,51]. By 2300, Antarctic ice loss contributes ~1.5 m to global mean sea-level rise in the moderate ice melt scenario and ~3.5 m in the high ice melt scenario. Both the moderate and high ice melt scenarios adopt the same Greenland ice melt trajectory, which contributes ~54 cm to global mean sea-level rise by 2300.

The Antarctic ice melt scenarios used in this study span much of the sea level contribution range projected by the Ice Sheet Model Intercomparison for CMIP6 (ISMIP6) ensemble, which suggests a sea level contribution between −37.4 cm and +62.2 cm under the low-emission pathway and between −0.6 m and +4.4 m under the high-emission pathway by 2300[9]. The adopted ice sheet simulations also show a spatial pattern and magnitude of retreat comparable to other Antarctic and Greenland ice sheet simulations[9,78,79]. More specifically, under the high-emission pathway, the adopted Antarctic ice sheet simulations predict significant retreat in West Antarctica and modest retreat elsewhere over the next three centuries, broadly matching other ISMIP6 simulations[9].

In our sea level calculations, we specifically used grounded ice, extracted from the ice height and bedrock topography fields provided in the ice sheet model output. Horizontal resolution in the SICOPOLIS ice sheet simulations is 8 km for Antarctica[51] and 5 km for Greenland[50], which is sufficient to capture grounding line migration dynamics[80,81].

Our estimates of land exposure do not account for sea-level changes resulting from ice loading changes following the Last Glacial Maximum (LGM). Estimates of relative sea-level change and vertical crustal motion associated with ice loading changes since the LGM differ widely in the literature[49,82–86], and there remains significant uncertainty in ice loading changes in Antarctica throughout the Late Pleistocene and Holocene[87–90]. Present-day vertical motion rates associated with ice loading changes since the LGM generally range from −3 mm yr^{-1} to 11 mm yr^{-1} (refs. 49,82–86). Over the ~300-year period considered in this study, these vertical crustal motion rates correspond to maximum of ~3 m of crustal deformation due to GIA from post-LGM ice loading changes.

Computing ice-free land exposure

We determined ice-free land exposure by adding modelled topography changes (negative sea-level changes) at selected times of interest to initial bedrock topography and checking that the area is both above sea level and free of grounded ice. Initial bedrock topography for the ice-free land exposure calculations is from the 30-arc-second-resolution (~1 km) ETOPO 2022 Global Relief Model[91], which adopts BedMachine bedrock topography in Antarctica[92]. The 30-arc-second-resolution initial bedrock topography, grounded ice extent (8 km resolution) and modelled sea-level changes (~4 km resolution) were all interpolated onto a common, near-uniform ~1 km spherical triangular grid covering the Antarctic domain to compute ice-free land area exposure at selected times of interest.

Furthermore, we defined a land mask operator on that grid acting on a field F:

$$M(F) = 1 \text{ if } F > 0 \tag{1}$$

$$M(F) = 0 \text{ if } F \leq 0 \tag{2}$$

where $M(F) = 1$ corresponds to ice-free land. At some time, t, the ice-free land mask can be expressed as

$$L(t) = M[T(t)] \times \{1 - M[\mathrm{IAF}(t)]\} \tag{3}$$

where T and IAF are topography and ice above flotation, respectively. The spatial extent of ice-free land changes, $\mathrm{d}L(t)$, with respect to the reference time, t_{ref}, at time t, is then simply:

$$\mathrm{d}L(t) = L(t) - L(t_{\mathrm{ref}}) \tag{4}$$

Note that $\mathrm{d}L > 0$ corresponds to a land gain resulting from either ice retreat or sea-level fall, while $\mathrm{d}L < 0$ corresponds to a land loss resulting from either ice advance or sea-level rise. To single out the contribution of sea-level change alone, $\mathrm{d}D(t)$, to the above expression at time t:

$$\mathrm{d}D(t) = \{M[T(t)] - M(t_{\mathrm{ref}})\} \times \{1 - M[\mathrm{IAF}(t)]\} \tag{5}$$

We show positive $\mathrm{d}D(t)$ in red in Figs. 3–6 and Extended Data Fig. 3–7. The difference $\mathrm{d}L(t) - \mathrm{d}D(t)$ is the contribution to ice-free land change due to ice retreat, shown in black in Figs. 3–6 and Extended Data Fig. 3–7.

To assess the sensitivity of our ice-free land emergence estimates to the resolution of the initial bedrock topography, we computed ice-free land emergence in 2300 for the high ice melt scenario using five different topography resolutions for the Antarctic Peninsula sector claimed by Argentina, Chile and the United Kingdom (Sector 8 in Fig. 5). We specifically computed land exposure using the ETOPO 2022 Global Relief Model at 15-arc-second (~0.5 km), 30-arc-second (~1 km) and 60-arc-second (~2 km) resolution. We also computed land exposure using the 8-km-resolution bedrock topography provided with the adopted Antarctic ice sheet models and a 4-km-resolution bedrock topography interpolated from the 60-arc-second ETOPO 2022 model. The bedrock topography resolution tests showed that higher grid resolution yields more accurate land exposure estimates in Sector 8 (Extended Data Table 3). However, calculating land exposure on

higher grid resolution comes with an increase in computational cost. To balance computational cost with land exposure calculation accuracy, we used 1-km-resolution bedrock topography for Antarctic-wide land exposure calculations throughout this study. Overall, the resolution tests indicate that ice sheet retreat and modelled sea-level changes primarily control ice-free land emergence estimates, rather than the resolution of the adopted bedrock topography.

Data availability

Ice-free land and sea-level change projections from this study are available via Dryad at https://doi.org/10.5061/dryad.f7m0cfz9j (ref. 93). Antarctic and Greenland ice sheet models[50,51] used for sea level projections can be accessed via Zenodo at https://doi.org/10.5281/zenodo.7773727 (ref. 94) and https://doi.org/10.5281/zenodo.5880517 (ref. 95), respectively. The ETOPO 2022 Global Relief Model used for ice-free land exposure calculations can be accessed at https://doi.org/10.25921/fd45-gt74 (ref. 96). The figures were generated using the Generic Mapping Tools[97] and ParaView[98].

Code availability

The code needed to reproduce the results and figures presented in this study is available via Zenodo at https://doi.org/10.5281/zenodo.7126141 (ref. 99). Procedures for reproducing the ice-free land emergence projections using the sea-level change projections and initial bedrock topography are outlined in the Methods.

References

67. Conrad, C. P. & Lithgow-Bertelloni, C. Influence of continental roots and asthenosphere on plate–mantle coupling. *Geophys. Res. Lett.* **33**, L05312 (2006).
68. Hay, C. C. et al. Sea level fingerprints in a region of complex Earth structure: the case of WAIS. *J. Clim.* **30**, 1881–1892 (2017).
69. Lucas, E. M., Gomez, N. & Wilson, T. The impact of regional-scale upper mantle heterogeneity on glacial isostatic adjustment in West Antarctica. *Cryosphere* **19**, 2387–2405 (2025a).
70. Lloyd, A. et al. Seismic structure of the Antarctic upper mantle imaged with adjoint tomography. *J. Geophys. Res. Solid Earth* https://doi.org/10.1029/2019JB017823 (2020).
71. Lei, W. et al. Global adjoint tomography—model GLAD-m25. *Geophys. J. Int.* **223**, 1–21 (2020).
72. Austermann, J., Mitrovica, J. X., Latychev, K. & Milne, G. A. Barbados-based estimate of ice volume at Last Glacial Maximum affected by subducted plate. *Nat. Geosci.* **6**, 553–557 (2013).
73. Kustowski, B., Ekström, G. & Dziewoński, A. Anisotropic shear-wave velocity structure of the Earth's mantle: a global model. *J. Geophys. Res. Solid Earth* **113**, B06306 (2008).
74. SICOPOLIS version 5-dev, branch develop, commit hash cb5a75b92 (GitLab, Alfred Wegener Institute for Polar and Marine Research, 2021); https://gitlab.awi.de/sicopolis/sicopolis
75. Eyring, V. et al. Overview of the Coupled Model Intercomparison Project Phase 6 (CMIP6) experimental design and organization. *Geosci. Model Dev.* **9**, 1937–1958 (2016).
76. Seroussi, H. et al. ISMIP6 Antarctica: a multi-model ensemble of the Antarctic ice sheet evolution over the 21st century. *Cryosphere* **14**, 3033–3070 (2020).
77. Nowicki, S. et al. Experimental protocol for sea level projections from ISMIP6 stand-alone ice sheet models. *Cryosphere* **14**, 2331–2368 (2020).
78. Goelzer, H. et al. The future sea-level contribution of the Greenland ice sheet: a multi-model ensemble study of ISMIP6. *Cryosphere* **14**, 3071–3096 (2020).
79. Aschwanden, A. et al. Contribution of the Greenland ice sheet to sea level over the next millennium. *Sci. Adv.* **5**, eaav9396 (2019).
80. Gladstone, R. M. et al. Marine ice sheet model performance depends on basal sliding physics and sub-shelf melting. *Cryosphere* **11**, 319–329 (2017).
81. Chambers, C., Greve, R., Obase, T., Saito, F. & Abe-Ouchi, A. Mass loss of the Antarctic ice sheet until the year 3000 under a sustained late-21st-century climate. *J. Glaciol.* **68**, 605–617 (2022).
82. Argus, D. F., Peltier, W. R., Drummond, R. & Moore, A. W. The Antarctica component of postglacial rebound model ICE-6G_C (VM5a) based on GPS positioning, exposure age dating of ice thicknesses, and relative sea level histories. *Geophys. J. Int.* **198**, 537–563 (2014).
83. van der Wal, W., Whitehouse, P. L. & Schrama, E. J. Effect of GIA models with 3D composite mantle viscosity on GRACE mass balance estimates for Antarctica. *Earth Planet. Sci. Lett.* **414**, 134–143 (2015).
84. Whitehouse, P. L., Bentley, M. J., Milne, G. A., King, M. A. & Thomas, I. D. A new glacial isostatic adjustment model for Antarctica: calibrated and tested using observations of relative sea-level change and present-day uplift rates. *Geophys. J. Int.* **190**, 1464–1482 (2012).
85. Ivins, E. R. et al. Antarctic contribution to sea-level rise observed by GRACE with improved GIA correction. *J. Geophys. Res. Solid Earth* **118**, 3126–3141 (2013).
86. Peltier, W., Argus, D. F. & Drummond, R. Space geodesy constrains ice age terminal deglaciation: the global ICE-6G_C (VM5a) model. *J. Geophys. Res. Solid Earth* **120**, 450–487 (2015).
87. Siegert, M., Ross, N., Corr, H., Kingslake, J. & Hindmarsh, R. Late Holocene ice-flow reconfiguration in the Weddell Sea sector of West Antarctica. *Quat. Sci. Rev.* **78**, 98–107 (2013).
88. Bradley, S. L., Hindmarsh, R. C. A., Whitehouse, P. L., Bentley, M. J. & King, M. A. Low post-glacial rebound rates in the Weddell Sea due to Late Holocene ice-sheet readvance. *Earth Planet. Sci. Lett.* **413**, 79–89 (2015).
89. Johnson, J. S. et al. Review article: existing and potential evidence for Holocene grounding line retreat and readvance in Antarctica. *Cryosphere* **16**, 1543–1562 (2022).
90. Balco, G. et al. Reversible ice sheet thinning in the Amundsen Sea Embayment during the Late Holocene. *Cryosphere* **17**, 1787–1801 (2023).
91. MacFerrin, M., Amante, C., Carignan, K., Love, M. & Lim, E. The Earth Topography 2022 (ETOPO 2022) global DEM dataset. *Earth Syst. Sci. Data* **17**, 1835–1849 (2025).
92. Morlighem, M. et al. Deep glacial troughs and stabilizing ridges unveiled beneath the margins of the Antarctic ice sheet. *Nat. Geosci.* **13**, 132–137 (2020).
93. Lucas, E. M. et al. Data from 'Emergence of Antarctic mineral resources in a warming world'. *Dryad* https://doi.org/10.5061/dryad.f7m0cfz9j (2026).
94. Greve, R. et al. Dataset for 'Future projections for the Antarctic ice sheet until the year 2300 with a climate-index method'. *Zenodo* https://doi.org/10.5281/zenodo.7773727 (2023).
95. Greve, R. & Chambers, C. Dataset for 'Mass loss of the Greenland ice sheet until the year 3000 under a sustained late-21st-century climate'. *Zenodo* https://doi.org/10.5281/zenodo.5880517 (2022).
96. *ETOPO 2022 15 Arc-Second Global Relief Model* (NOAA National Centers for Environmental Information, 2022); https://doi.org/10.25921/fd45-gt74
97. Wessel, P. et al. The Generic Mapping Tools version 6. *Geochem. Geophys. Geosyst.* **20**, 5556–5564 (2019).
98. Ahrens, J., Geveci, B. & Law, C. in *Visualization Handbook* (eds Hansen, C. D. & Johnson, C. R.) 717–731 (Elsevier, 2005).
99. Borreggine, M. et al. Sea-level rise in southwest Greenland as a contributor to Viking abandonment [data set]. *Zenodo* https://doi.org/10.5281/zenodo.7126141 (2023).

Acknowledgements
E.M.L. acknowledges support from Natural Sciences and Engineering Research Council of Canada grant no. RGPIN-2016-05159. J.X.M. acknowledges support from the National Science Foundation (NSF) grant OPP-2142593. This material is based on work supported by Harvard University (J.X.M., X.B. and G.C.). X.B. is supported by a Reginald A. Daly Postdoctoral Fellowship. M.J.H. acknowledges support from the Australian Research Council via a Discovery Early Career Researcher Award (no. DE220101519). F.D.R. was supported by the European Research Council under the European Union's Horizon 2020 research and innovation programme (grant agreement no. 101221058—Earth2Sea).

Author contributions
E.M.L., J.X.M., L.J.S.T. and K.L. conceptualized the project. E.M.L., J.X.M., K.L., F.D.R. and M.J.H. devised the methodology. All authors carried out the investigation. E.M.L., K.L., J.X.M. and F.D.R. visualized the results. J.X.M., M.J.H, X.B. and F.D.R. acquired the funding. E.M.L. and J.X.M. supervised the project. E.M.L., J.X.M., F.D.R., M.J.H., L.J.S.T., G.C. and S.R.J.T. wrote the original draft of the manuscript. All authors reviewed and edited the manuscript.

Competing interests
The authors declare no competing interests.

Additional information
Extended data is available for this paper at https://doi.org/10.1038/s41558-026-02569-1.

Correspondence and requests for materials should be addressed to Erica M. Lucas.

Peer review information *Nature Climate Change* thanks Simon Cox, Anthony Press and Andrew Shepherd for their contribution to the peer review of this work.

Reprints and permissions information is available at www.nature.com/reprints.

https://doi.org/10.1038/s41558-026-02569-1

Extended Data Table 1 | Land emergence for the high, moderate and low ice melt scenarios

	High ice melt		Moderate ice melt		Low ice melt	
Year	Total ice-free area change (km^2)	Ice-free area change from sea level change (km^2)	Total ice-free area change (km^2)	Ice-free area change from sea level change (km^2)	Total ice-free area change (km^2)	Ice-free area from sea level change (km^2)
2100	1,351	14	917	-9	29	-8
2150	6,136	1,261	1,424	35	223	32
2200	45,072	2,422	4,262	769	63	42
2250	75,231	3,512	15,272	1,533	161	52
2300	120,610	6,652	36,381	2,215	149	110

We include values for both the total change in ice-free area and the change in ice-free area resulting from sea level change for each ice melt scenario. Positive values indicate ice-free area gain, while negative values indicate ice-free area loss.

https://doi.org/10.1038/s41558-026-02569-1

Extended Data Table 2 | Land emergence by sectors with territorial claims for the high, moderate and low ice melt scenarios

	High ice melt			Moderate ice melt			Low ice melt		
Country	**2100**	**2200**	**2300**	**2100**	**2200**	**2300**	**2100**	**2200**	**2300**
Norway (1)	0	99	385	0	0	28	1	1	1
Australia (2)	284	3,124	16,843	239	562	994	134	92	191
France (3)	18	18	47	18	18	0	18	18	18
New Zealand (4)	322	967	13,511	177	438	628	14	-37	-86
Unclaimed (5)	775	3,328	14,315	389	454	1,085	-172	26	66
Chile (6)	2	2	25	2	2	9	2	-27	-27
Chile + UK (7)	-75	1,496	4,329	13	13	75	13	0	0
Argentina + Chile + UK (8)	27	36,043	70,992	79	2,776	33,542	20	-10	-14
Argentina + UK (9)	0	4	7	0	0	4	0	0	0
UK (10)	0	0	-54	0	0	0	0	0	0

The number following each country or group of countries in the first column corresponds to the numbering used in Fig. 5 and Extended Data Figs. 6, 7. Positive values indicate ice-free area gain, while negative values indicate ice-free area loss.

https://doi.org/10.1038/s41558-026-02569-1

Extended Data Table 3 | Sensitivity of ice-free land emergence estimates to topography grid resolution

Topography grid resolution	Number of grid points in sector 8 (Fig. 5)	Total ice-free area change (km^2)	Percent error relative to the bedrock topography grid with 0.5 km resolution
8 km	11,211	74,097	3.8%
4 km	36,702	69,408	2.8%
2 km	167,137	70,375	1.4%
1 km	637,260	71,053	0.5%
0.5 km	2,510,571	71,390	n/a

Results from topography resolution sensitivity tests performed for the high ice melt scenario in the Sector 8 of the Antarctic Peninsula (Fig. 5).

https://doi.org/10.1038/s41558-026-02569-1

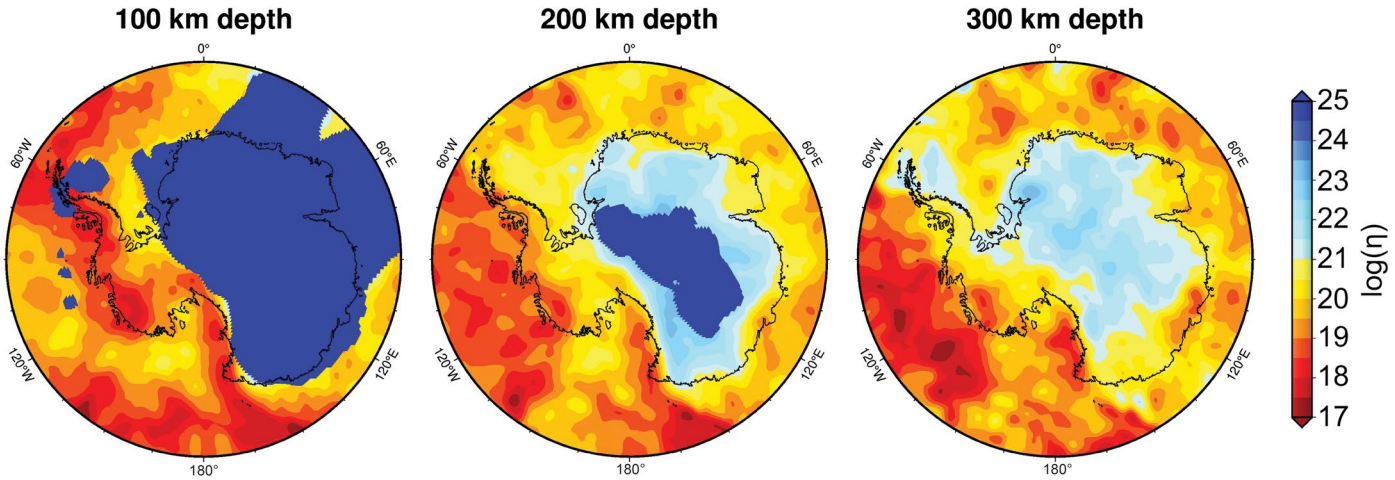

Extended Data Fig. 1 | 3-D Earth model used for GIA simulations. Mantle viscosity at 100 km, 200 km, and 300 km depth. The lithosphere, based on the model of (66), extending to 100 km and 200 km depth is shown in saturated dark blue.

https://doi.org/10.1038/s41558-026-02569-1

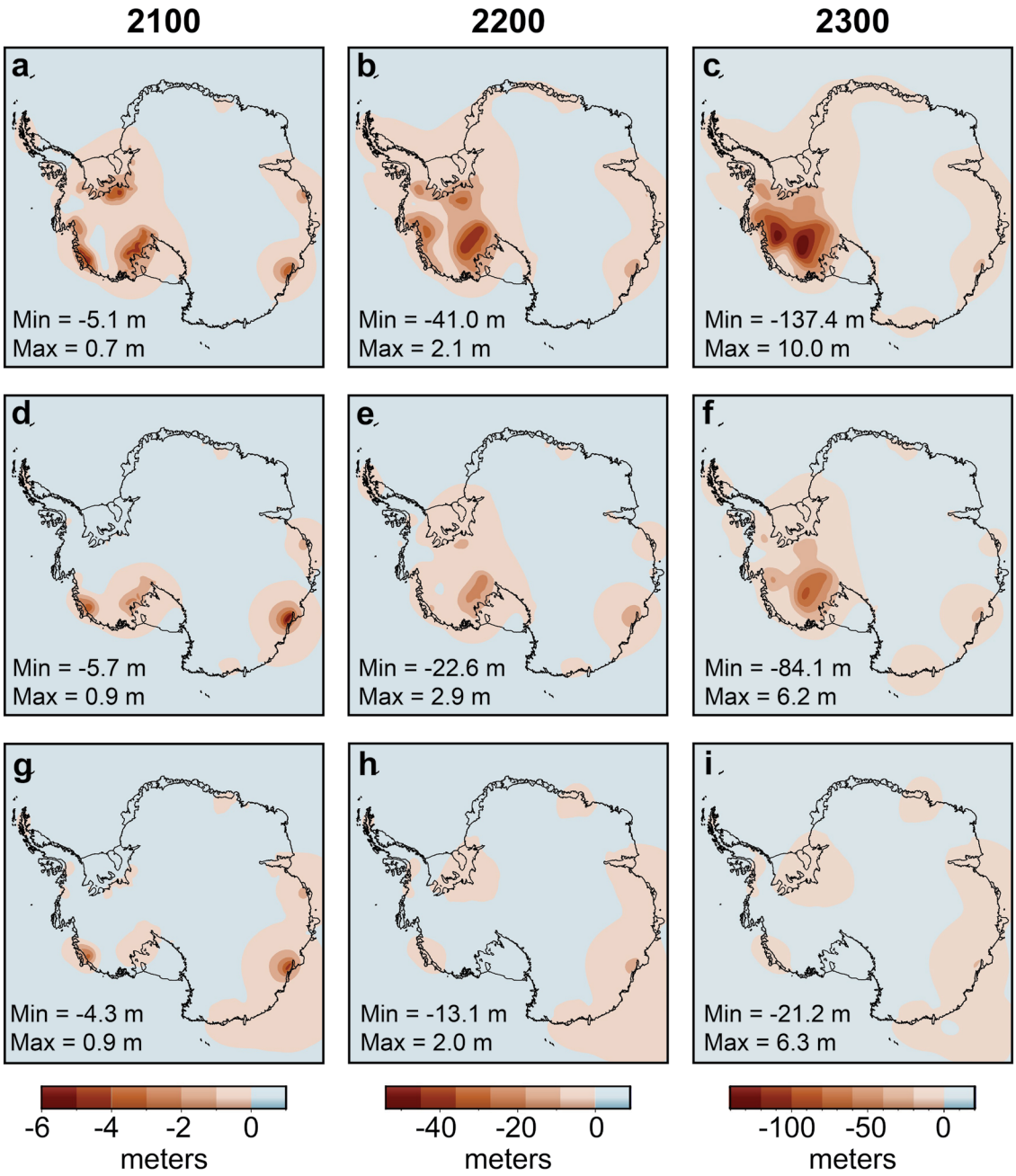

Extended Data Fig. 2 | Relative sea level change projections. Relative sea level change in 2100, 2200, and 2300 with respect to 2015 for the **a**-**c** high, **d**-**f** moderate, and **g**-**i** low ice melt scenarios.

https://doi.org/10.1038/s41558-026-02569-1

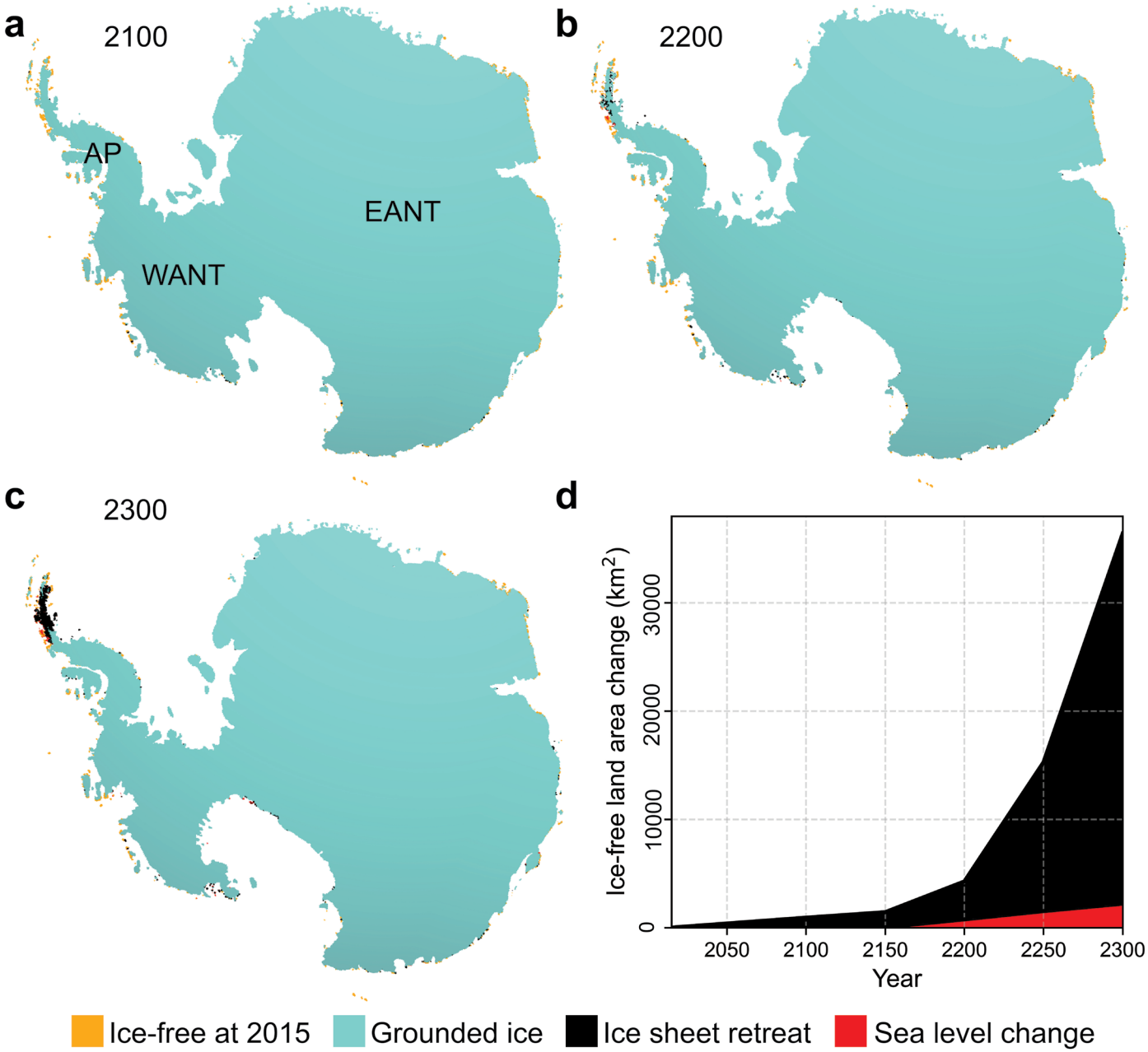

Extended Data Fig. 3 | Land emergence for the moderate ice melt scenario. **a**-**c**, Projections of land emergence due to ice sheet retreat and sea level change for 2100, 2200, and 2300. Land area in 2015, calculated from the initial ice sheet extent of the adopted ice sheet model and high-resolution bedrock topography, is also plotted. **d**, Total ice-free area gains from 2015 through 2300. The contributions from ice sheet retreat and sea level change are plotted in black and red, respectively. Extended Data Fig. 5 provides higher resolution plots in select regions for 2300.

https://doi.org/10.1038/s41558-026-02569-1

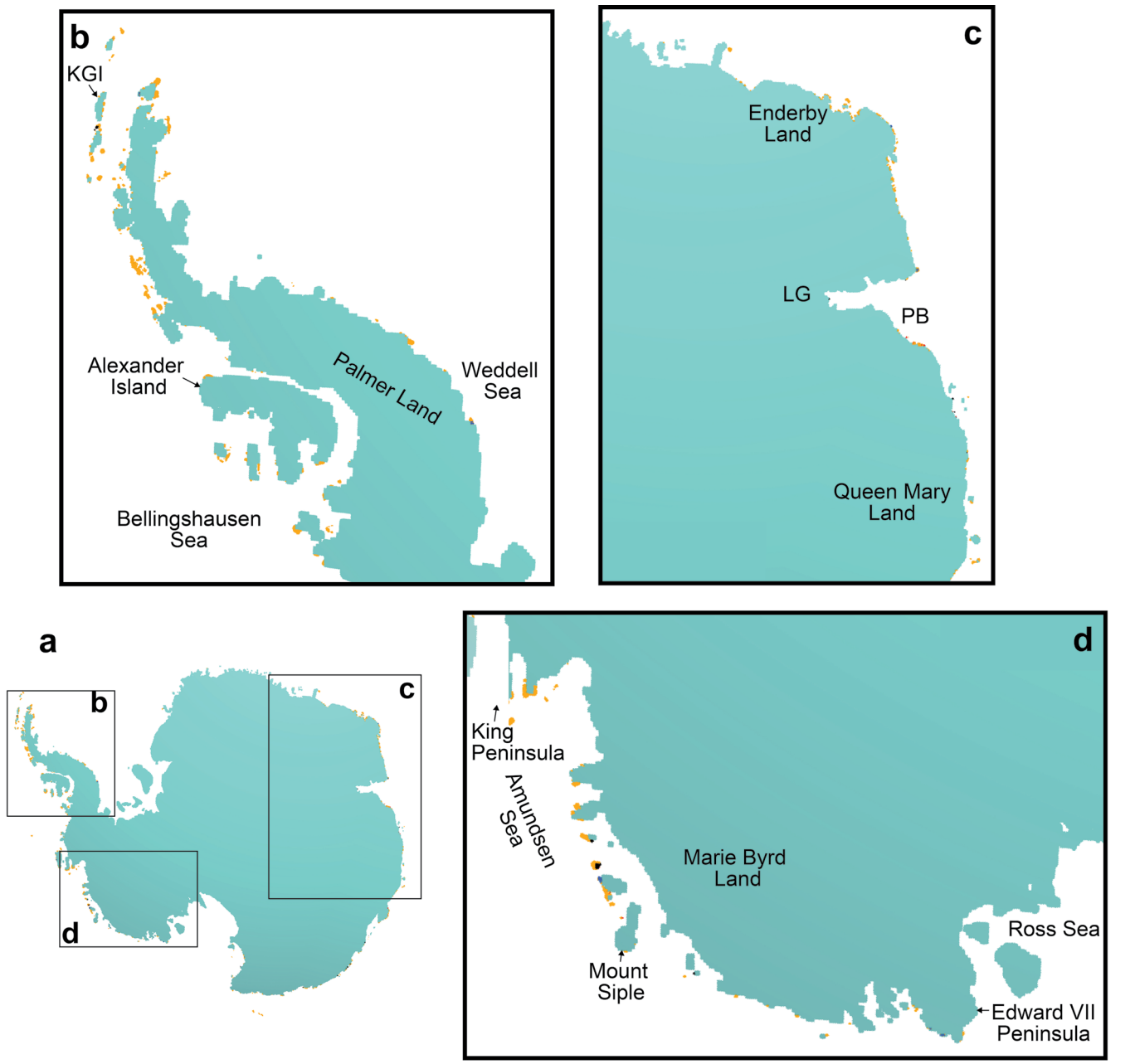

Extended Data Fig. 4 | Regional-scale view of Land emergence by 2300 for the low ice melt scenario. a, Map delineating regions shown in **b**-**d**. **b**, Ice-free land in the Antarctic Peninsula at 2300. **c**, Land emergence in a coastal sector of East Antarctica, with the Lambert Graben (LG) and Prydz Bay (PB) labelled. **d**, Land emergence in the Ross Sea, Amundsen Sea, and Marie Byrd Land sectors of West Antarctica.

https://doi.org/10.1038/s41558-026-02569-1

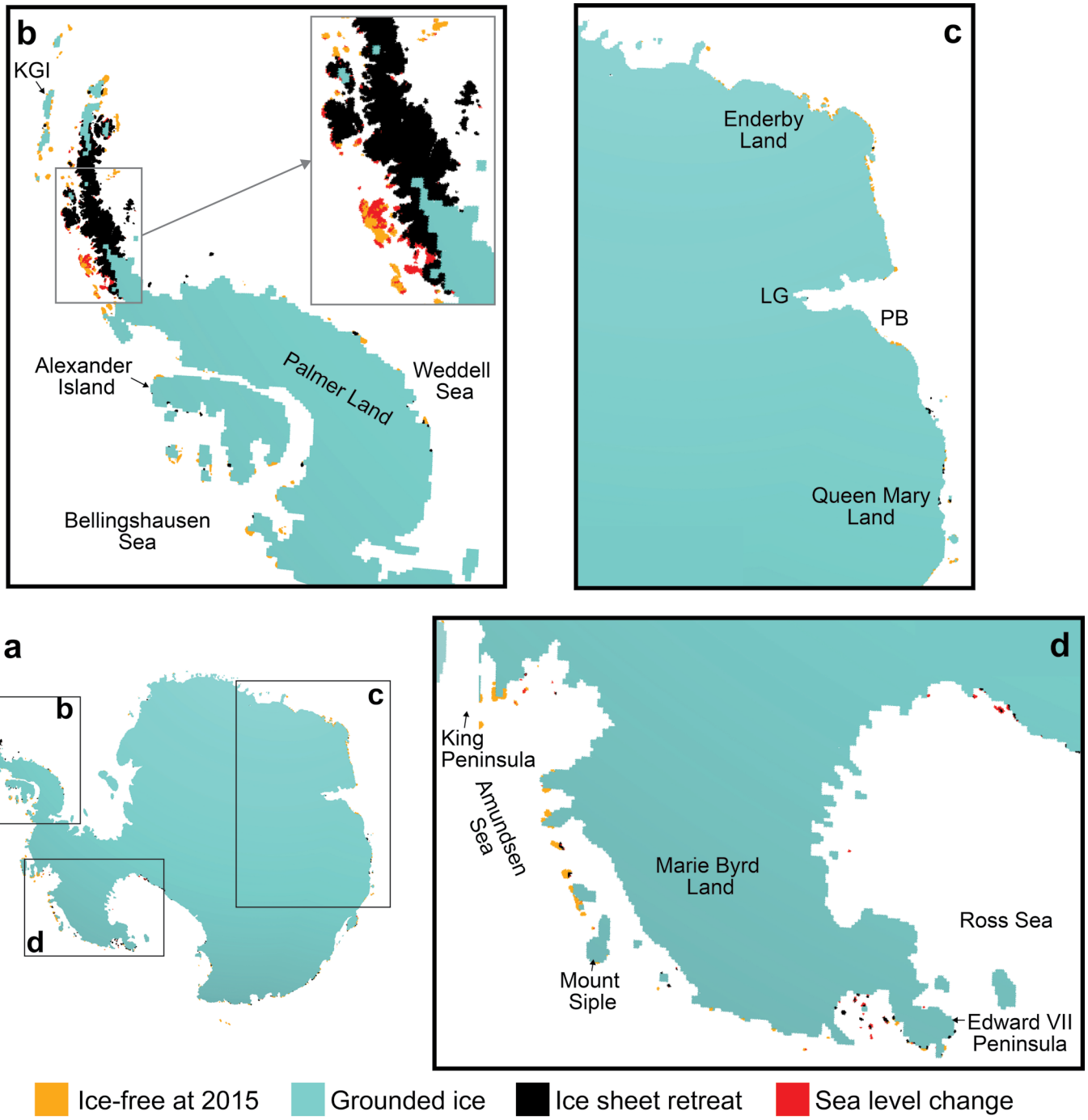

Extended Data Fig. 5 | Regional-scale view of land emergence by 2300 for the moderate ice melt scenario. a, Map delineating regions shown in **b**-**d**. **b**, Ice-free land in the Antarctic Peninsula at 2300. King George Island (KGI) is labeled. **c**, Land emergence in a coastal sector of East Antarctica, with the Lambert Graben (LG) and Prydz Bay (PB) labelled. **d**, Land emergence in the Ross Sea, Amundsen Sea, and Marie Byrd Land sectors of West Antarctica.

https://doi.org/10.1038/s41558-026-02569-1

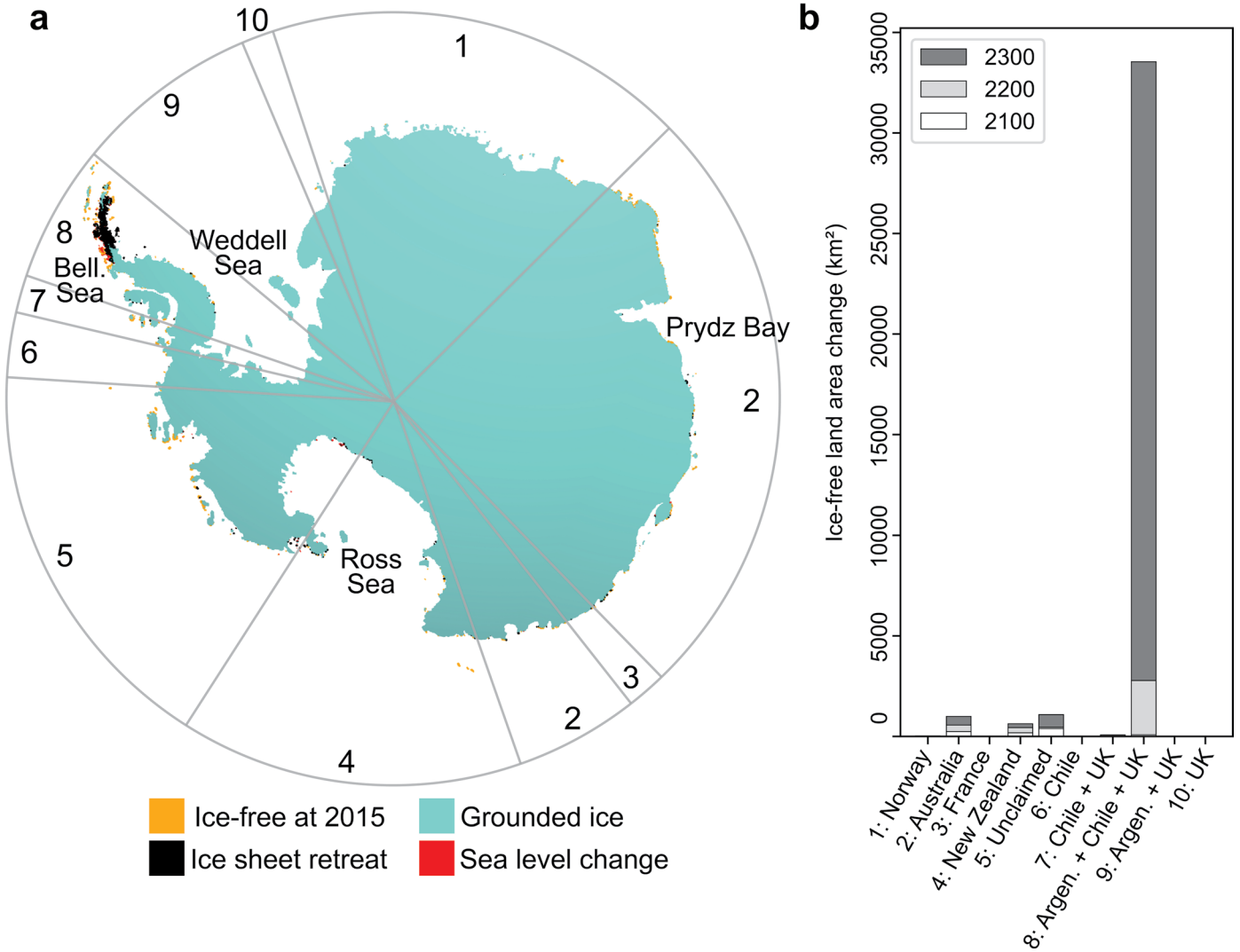

Extended Data Fig. 6 | Land emergence in claimed territories for the moderate ice melt scenario. a, Land exposed at 2300 for the moderate ice melt scenario. Gray lines delineate sectors with territorial claims; numbers 1 through 10 correspond to countries or groups of countries labeled in the bar chart in **b**. **b**, Land emergence by sector for 2100, 2200, and 2300.

https://doi.org/10.1038/s41558-026-02569-1

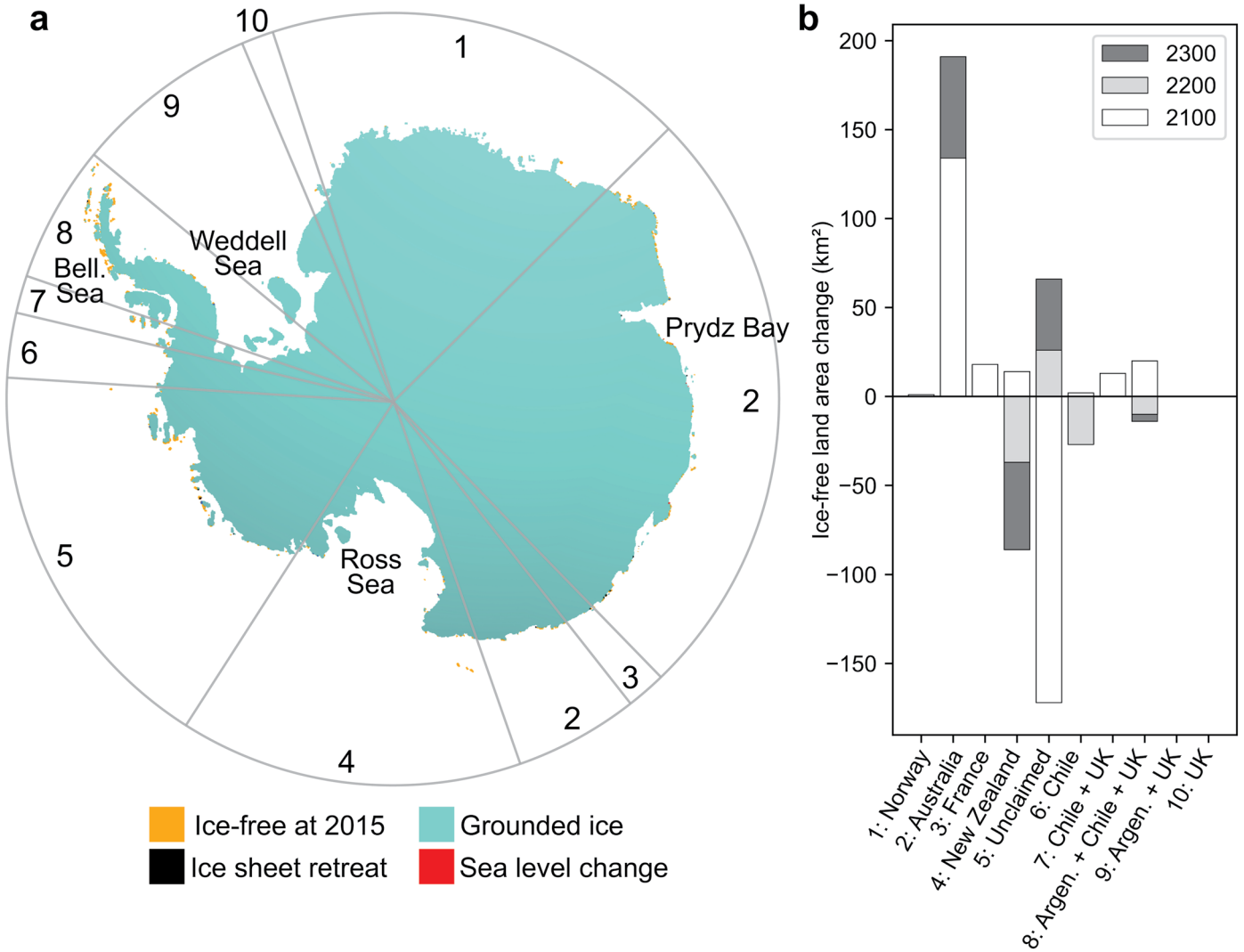

Extended Data Fig. 7 | Land emergence in claimed territories for the low ice melt scenario. a, Land exposed at 2300 for the low ice melt scenario. Gray lines delineate sectors with territorial claims; numbers 1 through 10 correspond to countries or groups of countries labeled in the bar chart in **b**. **b**, Land emergence by sector for 2100, 2200, and 2300.